A Recursive Computational Approach for Determining Axial Forces in Straight-walled Arch Tunnel Linings, Accounting for Elastic Resistance Influences

Rongbin Huang*, Hongbing Guo

Abstract—A comprehensive investigation into the stress distributions within straight-walled arched tunnel linings is essential for both the design of reinforcing structures and the evaluation of tunnel stability. In this research, we adopt an elliptical representation to characterize the curvature of the straight-walled arch apex, thereby establishing the basis for subsequent mechanical analysis. This framework is designed to identify potential instability zones, facilitating comprehensive evaluations of the tunnel lining's long-term durability. We present a recursive computational framework to quantitatively characterize the spatial heterogeneity and magnitude of elastic stiffness in tunnel linings. To optimize recursive computations, an iterative transfer coefficient (K) is introduced, significantly enhancing the efficiency and accuracy of internal force calculations within the lining. Through detailed calculations and comparative assessments, the practicality and superiority of our approach are demonstrated, providing a robust foundation for tunnel lining stability evaluations.

Index Terms—Straight-walled arch tunnel, stress analysis, elastic resistance, iterative calculation, iteration rate

I. INTRODUCTION

A thorough analysis of stress profiles in tunnel linings is crucial for designing support systems and undertaking stability evaluations, as documented in previous studies [1-3]. The precise quantification of elastic resistance distribution patterns remains a critical challenge in the mechanical analysis of straight-wall arch tunnel linings, particularly regarding the coupling effects between structural stiffness and surrounding rock deformation.

Regarding the computation of underground structures, two primary methodologies can be distinguished: stress-structure approach and stratigraphic-structure technique [4-5]. Under the assumption that stratum-lining interaction is exclusively

Manuscript received April 29, 2025; revised August 26, 2025.

This study is supported by (1) The Youth Innovation Team of Shaanxi Universitie, No. 24JP017; (2) 2023 Shaanxi Transportation Vocational and Technical College Research Innovation Team Funding Project; (3) Natural Science Basic Research Program of Shaanxi Province, No. 2024JC-YBQN-0609; (4) Key Research Projects for Shaanxi Higher Education Teaching Reform in 2023, No.23GG010.

Rongbin Huang is a lecturer of Shaanxi College of Communications Technology, Xi'an 710018, China. (corresponding author to provide e-mail: rbhuang2024@163.com).

Hongbing Guo is a professor of Shaanxi College of Communications Technology, Xi'an 710018, China. (e-mail: SJYTG2024@163.com).

mediated through force application mechanisms—including active earth pressure from the surrounding strata and passive elastic restraint—the load-transfer methodology functions within a quasi-static equilibrium framework, wherein the spatial distribution of interfacial forces adheres to the principle of minimum complementary energy [6-8]. This methodology's simplicity in terms of mechanical modeling facilitates its practical application and ease of implementation in engineering contexts. Over the past century, sophisticated theoretical frameworks have emerged within the load-structure method [12-13].

However, when employing the stress-structure analytical approach for straight-walled arch tunnel linings, the accurate quantification of elastic restraint coefficients constitutes a decisive factor in structural reliability assessment. Traditionally, this has involved forming initial hypotheses and iteratively refining them. The selected distribution format and approximation technique critically influence both computational While proficiency and precision. project-specific measurement data has been harnessed in some studies to ascertain elastic restraint, these findings lack broad applicability [14-15].

In our ongoing research endeavors, we have chosen to employ the load-structure method for the computation of the stress distributions. The primary objective of adopting this method is to identify the most vulnerable zones within the lining that may potentially compromise its long-term stability. This comprehensive analysis will serve as a foundational cornerstone for conducting rigorous stability evaluations and ensuring the structural integrity of the tunnel. The novelty of this study is as follows: In the calculation process, it was first proposed to use ellipses as fitting curves for tunnel arch sections. This method provides greater flexibility in adapting to tunnels with different height span ratios and greatly reduces errors that may occur due to selecting inappropriate cross-sectional shapes. Concurrently, an iterative algorithm is implemented to determine the spatial distribution and magnitude range of elastic restraint. A novel iterative transfer coefficient K is proposed herein to streamline the convergence process, thereby enabling both computational efficiency and high-precision determination of lining internal forces.

II. MATERIALS AND METHODS

The present study proposes the employment of an elliptical contour to approximate the cross-sectional profile of

straight-walled arch tunnels characterized by a significant difference between their height and width. This approximation technique constitutes the cornerstone for evaluating the internal forces within the tunnel lining. Illustration 1 showcases the cross-sectional approximation for such tunnels.

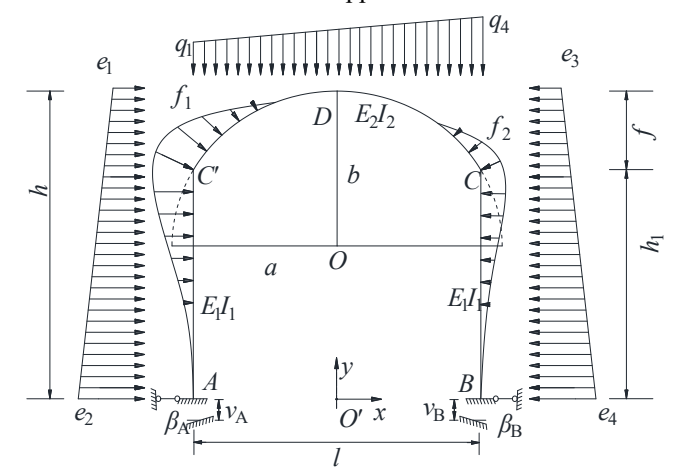


Fig. 1. Schematic representation of the mechanical calculation model

In Fig 1, we find a series of symbols that are meticulously defined for clarity. Specifically, A and B serve as indicators for the tunnel lining's left and right arch supports, respectively. The tunnel span (designated as CC') is operationally defined as the horizontal chord length connecting the outermost extremities of the tunnel's sidewalls, measured along the principal axis of symmetry of the cross-sectional geometry. Moving upwards, we encounter the tunnel apex, denoted by D, a crucial point where the tunnel vault intersects with the ellipse's superior vertex. Additionally, the ellipse's centroid is designated with the symbol O, while O' marks the origin of the coordinate system, providing a reference point for our measurements.

Furthermore, the ellipse's left semi-major axis and upper semi-minor axis are identified with the lengths a and b, respectively, offering insights into the ellipse's shape and size. Meanwhile, the symbol h is introduced to represent the tunnel's vertical extent, which spans from the tunnel floor to the vault's summit, giving us a sense of the tunnel's overall height.

With these symbols in place, we propose an elliptical approximation curve that skillfully traverses through points C, C', and D. This curve serves as a useful tool for modeling the tunnel's shape and dimensions. Below, we will delve into the details of how this elliptical approximation curve's formula is derived, providing a comprehensive understanding of its construction and application.

$$\frac{x^2}{a^2} + \frac{\left[y - (h - b)\right]^2}{b^2} = 1 \tag{1}$$

The discussed model exhibits a mirror-image arrangement, making it possible to bisect the tunnel precisely at vault midpoint D, yielding two identical primary constituents. Utilizing these primary constituents, one can adopt the equilibrium of forces principle to deduce the stress distribution pattern and deformation attributes of the lining, while accounting for the combined actions of geological forces, elastic limitations, and their mutual engagements.

A. Estimation of Internal Forces in Tunnel Lining Subject to Stratum Loads

At the tunnel vault's apex, designated as D, the cross-sectional profile is divided into two curved beams that cantilever outward, functioning as the primary structural elements. A simplified schematic representation of this configuration is illustrated in Figure 2, thereby aiding in the calculation process.

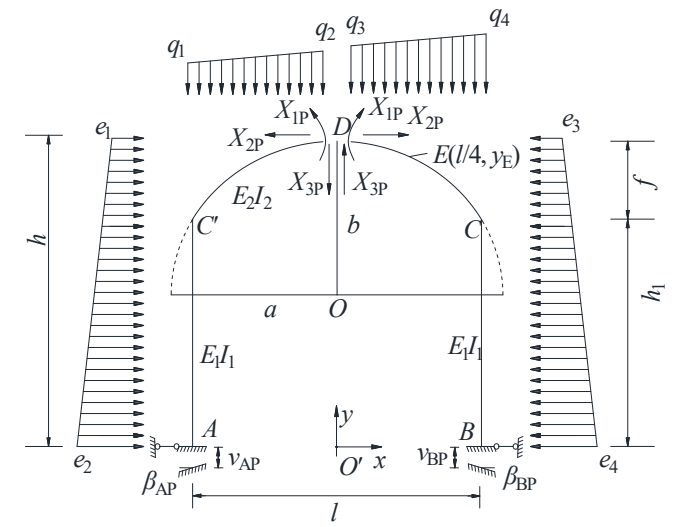


Fig. 2. Simplified schematic for assessing internal forces in tunnel lining subject to stratum loads

Upon examining the specific conditions at the apex of the tunnel vault, characterized by the absence of relative rotational angle, radial deformation, and tangential displacement, it is possible to derive the deformation compatibility equations. A simplified schematic of this configuration is provided in Fig 2, which facilitates the calculation process.

$$2\delta_{11}X_{1P} + 2\delta_{12}X_{2P} + \Delta_{1P}^{L} + \Delta_{1P}^{R} + \beta_{AP} + \beta_{BP} = 0$$

$$2\delta_{21}X_{1P} + 2\delta_{22}X_{2P} + \Delta_{2P}^{L} + \Delta_{2P}^{R} - u_{AP} - u_{BP} + h(\beta_{AP} + \beta_{BP}) = 0$$

$$2\delta_{33}X_{3P} + \Delta_{3P}^{L} + \Delta_{3P}^{R} + v_{AP} - v_{BP} + \frac{l}{2}(\beta_{BP} - \beta_{AP}) = 0$$

$$(2)$$

In the proposed constitutive model, δ_{ij} (i = 1,2,3; j = 1,2,3) is defined as the flexibility coefficient of the top of the straight-wall arch tunnel, representing the displacement component along the principal loading direction (X_{iP}) induced by a unit magnitude force (X_{jP} =1) applied to the structural system. Δ^{L}_{iP} , Δ^{R}_{iP} represent the displacements in the direction of force D that result from external loads. u_{AP} , v_{AP} and β_{AP} correspond to the horizontal, vertical, and rotational displacements, respectively, at point A. Correspondingly, u_{BP} , v_{BP} , and β_{BP} are designated as the horizontal displacement components at nodal point B along the principal coordinate axes (X, Y, and Z respectively), where these vector quantities represent the translational responses of the structural system.

Based on the principle of virtual work, a system of three equilibrium equations is established in Eq. (2) to determine the unknown generalized forces X_{1P} , X_{2P} , and X_{3P} through constrained optimization. The substitution of the obtained solutions facilitates the computation of the internal forces within the tunnel lining at any location subject to stratum pressure.

B. Assessment of Internal Stresses within Tunnel Linings under Elastic Constraints

In the process of evaluation, cantilevered curved beams serve as the cornerstone of our structural model, with a streamlined computational approach illustrated in Figure 2. This graphical representation delineates entities f_1 and f_2 , representing the elastic forces exerted on the lining's left and right flanks, respectively, in accordance with the prescribed equations of relationship.

$$\begin{cases}
f_1 = ku^L(y) \\
f_2 = ku^R(y)
\end{cases} \tag{3}$$

Within the established constitutive equations, the parameter k is defined as the elastic stiffness coefficient, while $u^L(y)$ and $u^R(y)$ respectively characterize the deformation responses of the tunnel lining's left and right structural flanks under load-bearing conditions. A visual representation of the model, which exclusively calculates the internal stresses within tunnel linings under the influence of elastic stiffness, can be found in Fig 3.

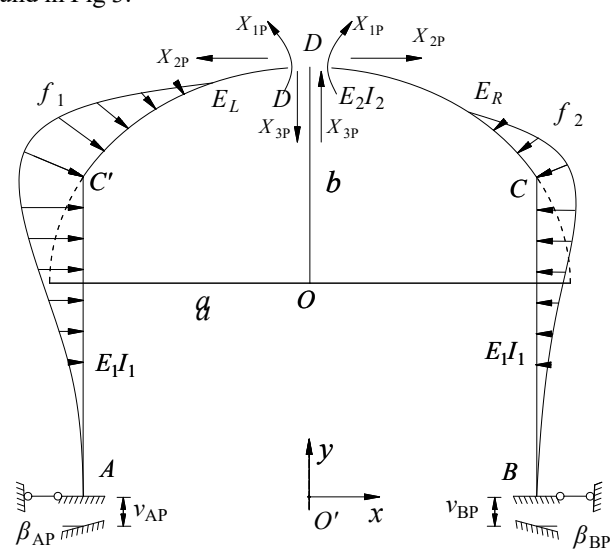


Fig. 3. Internal force model of tunnel lining under elastic resistance

At the center point D located atop the tunnel's arch, where the rotational angle, radial displacement, and tangential deflection are all zero, the corresponding deformation compatibility equation is formulated.

$$2\delta_{11}X_{1f} + 2\delta_{12}X_{2f} + \Delta_{1f}^{L} + \Delta_{1f}^{R} + \beta_{Af} + \beta_{Bf} = 0$$

$$2\delta_{21}X_{1f} + 2\delta_{22}X_{2f} + \Delta_{2f}^{L} + \Delta_{2f}^{R} - u_{Af} - u_{Bf} + h(\beta_{Af} + \beta_{Bf}) = 0$$

$$2\delta_{33}X_{3f} + \Delta_{3f}^{L} + \Delta_{3f}^{R} + v_{Af} - v_{Bf} + \frac{l}{2}(\beta_{Bf} - \beta_{Af}) = 0$$

$$(4)$$

Utilizing the principle of virtual work aids in identifying the parameters within Equation (4), which encompasses three equations, each corresponding to one of the three unknown variables. By substituting the solutions obtained, the internal

forces within the tunnel lining can be deduced under conditions of elastic stiffness.

C. Tunnel Lining Forces under Combined Pressures and Stiffness

As loads are applied and deformation occurs in a coordinated manner, the tunnel lining experiences variations in elastic stiffness that are directly proportional to its radial deformation. To accurately analyze the forces acting on the support structure, it is imperative to ascertain the distribution pattern of elastic stiffness. In this study, we employ an iterative computational approach to progressively align the elastic stiffness distribution with the lining deformation distribution, thereby ensuring precise elastic stiffness calculations. The iterative procedure for computing elastic stiffness involves the subsequent steps:

(1) Ascertainment of Lining Deformation Under External Loading

By employing the computational methodology outlined in Section 2, deformation values for various segments of a straight-wall arch tunnel lining, subjected to stratum pressure, can be accurately determined, with consideration given to both the material properties and structural configuration of the lining.

(2) Initial Iteration for Elastic Stiffness Computation

Using the lining deformation obtained under stratum pressure as the initial iteration point $u_{i=1}$, we determine the maximum deformation $u_{i=1}$ (max) across the entire lining cross-section, where i represents the iteration index. Utilizing the local deformation theory, the elastic stiffness is formulated as a function of the lining stiffness constant, denoted as $f_{i=1} = ku_{i=1}$. This equation facilitates the determination of both the magnitude and spatial distribution of the elastic stiffness.

(3) Second Iteration for Refinement of Elastic Stiffness Computation

Considering the combined effects of the external load P and the elastic stiffness $f_{i=1}$ obtained from the first iteration, we ascertain the second iteration lining deformation curve $u_{i=2}$ and its corresponding maximum deformation $u_{i=2} \, (\max)$. Furthermore, we compute the discrepancy χ_{1-2} between the maximum deformation values from consecutive iterations, expressed as:

$$\chi_{1-2} = |u_{i-2}(\max) - u_{i-1}(\max)|$$
 (5)

If the value of χ_{l-2} drops beneath the specified threshold $\overline{\chi}$, it indicates that the computations have achieved the necessary precision, thus triggering the cessation of additional calculations.

(4) The nth Iteration: Determination of Equilibrium Elastic Resistance Distribution

Reapply computational procedures using combined P and previous fn-1 for nth iteration, yielding lining displacement u_n . Concurrently, an evaluation is conducted to ascertain whether the nth iteration satisfies the prescribed accuracy benchmarks. Guided by this flowchart, MATLAB

programming is leveraged to expedite computer-assisted calculations.

To accelerate convergence in iterations, an adjustment factor K is introduced. The method for determining an appropriate K value is as follows:

$$\begin{cases} K_{i} = \left| \frac{u_{i-1}(\max) + u_{i-2}(\max)}{2u_{i-1}} \right|, & (i > 1) \\ K_{i} = 1, & (i = 1) \end{cases}$$

III. ENGINEERING CASE ANALYSIS

Taking the Tangjiayuan Tunnel in Shaanxi Province as an engineering example, conduct stress analysis on the tunnel. The main parameters of the tunnel are as follows.

Elastic Resistance Factor of Adjacent Rock Mass: k = 150MPa/m

In-situ Vertical Geostatic Stress Field in Tunnel Vicinity: $q_1 = 94.45 \, \text{kN/m}$, $q_2 = q_3 = 192 \, \text{kN/m}$, $q_4 = 289.55 \, \text{kN/m}$ Lateral Pressure Coefficient: $\lambda = 0.44$

Horizontal Rock Pressure on the Left Side: $e_3 = 41.56 \text{kN/m}$, $e_4 = 115.9 \text{kN/m}$.

Horizontal Rock Pressure on the Right Side: $e_1 = 127.4 \text{kN/m}$, $e_2 = 201.74 \text{kN/m}$.

Tunnel Cross-Sectional Dimensions: h = 10.39 m, a = 8.37 m, b = 7.51 m, $h_1 = 6.21 \text{m}$, l = 15 m, d = 0.6 m, $E = 2 \times 10^4 \text{ MPa}$, $I = 0.018 \text{m}^2$.

As illustrated in Figures 4 and 5, the absence of the iteration coefficient K induces a progressively decelerated convergence rate in successive iterations. Despite 31 iterations, the desired level of calculation accuracy remains elusive. K helps reach accuracy in seven iterations, giving precise lining displacements and elastic resistance. It uses medians of last two iterations for next displacement, keeping resistance accurate, optimizing calculations. Under the revised iteration protocol, the iterative computation of elastic reaction forces undergoes a notable enhancement in computational efficiency.

IV. DISCUSSION

To validate the computational accuracy of the proposed theoretical framework, comparative analyses were conducted between the presented methodology, numerical simulation techniques, and conventional analytical approaches using representative engineering case studies. The verification process is systematically elaborated as follows.

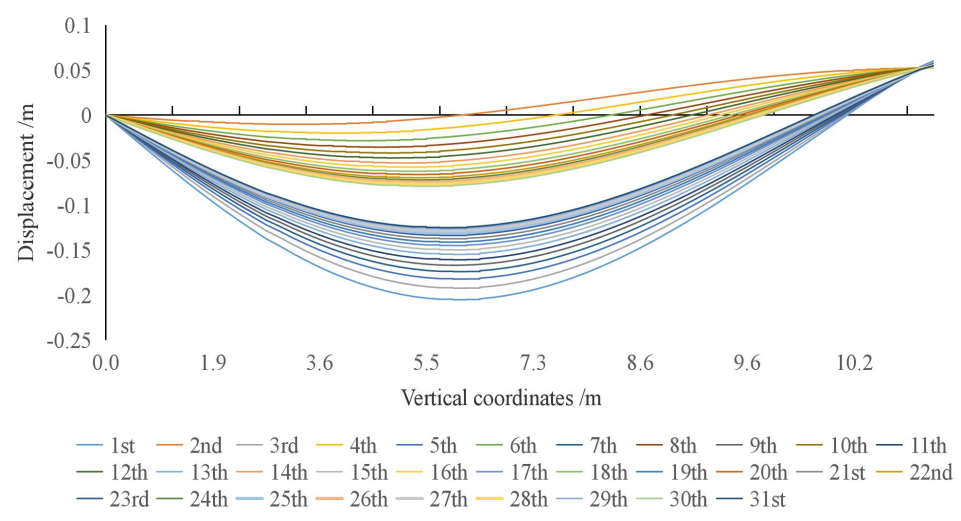


Fig. 4. Presents an iterative calculation of lining displacement without the incorporation of an iteration coefficient

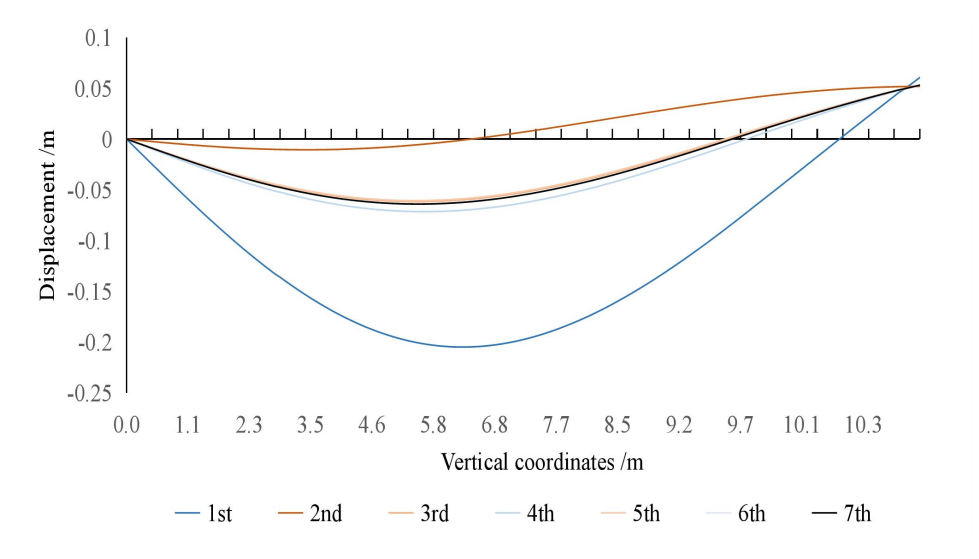


Fig. 5. Displays the iterative computation of lining displacement subsequent to the introduction of the iteration coefficient K

IAENG International Journal of Applied Mathematics

Use ANSYS software to perform numerical simulation calculations on tunnels. By combining theoretical calculations with simulation results, a comprehensive understanding and evaluation of the integrity of tunnel structures have been ensured. Furthermore, cross-validation between theoretical predictions and numerical simulations demonstrates the proposed method's computational accuracy with quantified error margins.

In this study, a spring system model was developed in ANSYS to simulate the elastic behavior of straight-wall arch linings, where structural components were discretized and interconnected via translational/rotational spring elements.

Constraints were imposed at the base of the structure in both X and Y directions. Since soil layers are incapable of exerting tensile forces on the segments, the model was refined by excluding tensile springs to improve its precision. To determine the range of elastic resistance distribution, iterative refinement techniques were employed. The computed results are depicted in Fig 6.

An analysis of stresses within the straight-wall arch tunnel, depicted in Fig 6, was performed and subsequently benchmarked against the theoretical calculations presented herein. The outcomes of this comparative analysis are summarized in Table I.

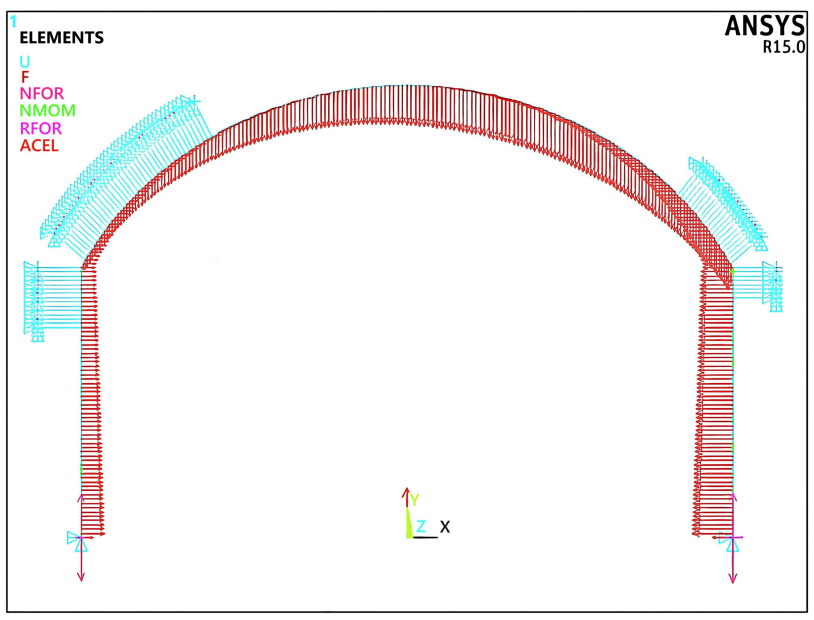


Fig. 6. Distribution range of elastic resistance modeled by spring elements

TABLE I
PRESENTS A COMPARATIVE ASSESSMENT OF THE CALCULATION OUTCOMES

			Midpoint of Left Wall	Vertex of Left Wall	Center of Left Arch	Center of Arch
Axial Force (kN)	ANSYS		2038.312	1996.541	1743.852	1613.744
	Theory Presented Herein		2038.478	1996.397	1743.695	1612.892
	Difference Value		0.166	0.144	0.157	0.852
Shear Force (kN)	ANSYS		67.929	679.720	2.629	72.490
	Theory Presented Herein		67.623	679.921	3.011	72.195
	Difference Value		0.306	0.201	0.282	0.295
$\begin{array}{c} \text{Bending} \\ \text{Moment} \left(k \textbf{N} \cdot \textbf{m} \right) \end{array}$	ANSYS		296.368	476.088	153.408	187.148
	Theory Presented Herein		296.105	475.852	153.093	186.971
	Difference Value		0.263	0.236	0.315	0.177
Deformation Magnitude (mm)	X-Direction	ANSYS	3.5628	3.5506	3.7502	2.6103
		Theory Presented Herein	3.6538	3.0786	4.0352	2.6043
		Difference Value	0.091	-0.472	0.285	-0.006
	Y-Direction	ANSYS	0.62988	1.2635	3.5012	12.022
		Theory Presented Herein	0.78188	1.4585	3.8852	11.931
		Difference Value	0.152	0.195	0.384	-0.091

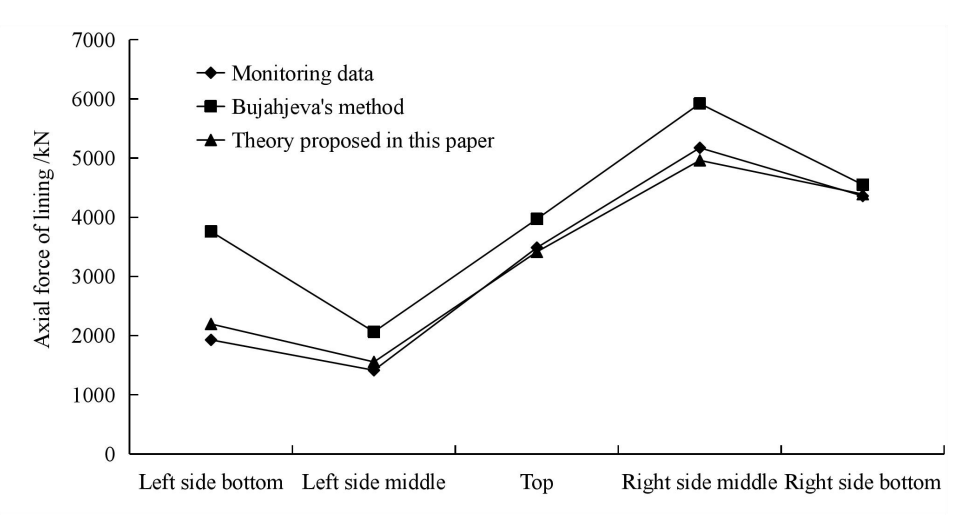


Fig. 7. Comparison of calculated axial forces of lining with monitoring data

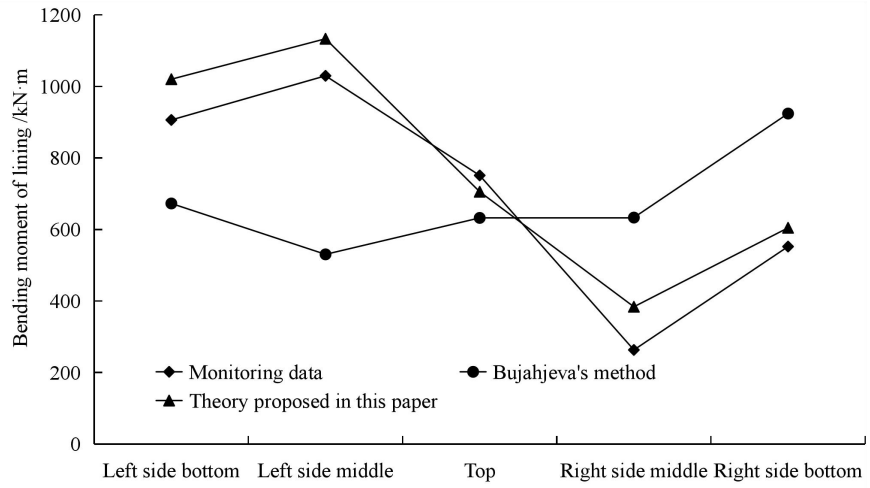


Fig. 8. Comparison of calculated bending moments of lining with monitoring data

As shown in Table I, the comparative analysis reveals the following quantified deviations: (a) Maximum axial force deviation of 0.852 kN (0.53% relative error); (b) Peak shear force discrepancy of 0.295 kN (0.5% relative error); (c) Maximal bending moment error of 0.315 kN·m (0.2% relative error); and (d) Deformation variations ranging from 0.09 mm to 0.472 mm. These results corroborate the strong alignment between the theoretical calculations presented in this study and the outcomes derived from ANSYS finite element analysis, thereby affirming the precision and dependability of the proposed theoretical model.

Bujahjeva's method is a commonly used calculation method for tunnel elastic resistance [16]. To validate the theoretical accuracy of the tunnel lining internal force calculation method proposed herein, comparative analyses were conducted using both Bujahjeva's classical method and the proposed theoretical framework for the Tangjiayuan Tunnel lining structure. Field-measured data were systematically incorporated to establish a comprehensive verification basis. The resultant force distributions obtained from the three approaches are quantitatively presented in Figure 7 and Figure 8.

The computational analysis demonstrates that the maximum relative deviations between the calculated axial forces obtained by the cloth method and the proposed theoretical model compared to field measurements are 94.9% and 13.9%, respectively. The maximum relative errors between the bending moments calculated by the two methods and the

measured data are 140.5% and 12.6%. At the same time, the curve obtained by the theory described in the paper is closer to the measured curve. It can be seen that the theory described in the paper can more accurately reflect the change law of internal force of curved wall arch lining in different positions.

During the discussion, calculations were performed using the theory proposed in this paper, numerical simulations, and traditionally used computational theories. The aforementioned calculation results were then compared and analyzed with on-site monitoring results. It was found that the theoretical calculation results presented in this paper were closer to the actual measured results, thus providing a more accurate representation of the actual stress conditions in the tunnel.

V.CONCLUSION

- (1) For the first time, an elliptical fitting method was proposed to characterize the cross-section of the arch crown in straight-wall arched tunnels. The centroid of the tunnel is located at the midpoint of the span line, where the semi-major and semi-minor axes of the ellipse are determined by measuring the distances from the centroid to both sidewall lining centerlines and the arch crown. Based on this fitted geometry, the internal forces of the secondary lining were calculated through structural analysis.
- (2) In the implementation of the proposed iterative method, the concept of iterative transfer coefficient (K) was first introduced, which significantly improved computational

efficiency and enhanced the practical applicability of the theoretical framework.

- (3) The theory presented in this paper is applied to analyze the stress and deformation of tunnels, and comparative analysis is conducted with numerical simulation, traditional theory, and on-site monitoring data. The comparison results indicate that the theoretical calculation results proposed in this paper are closer to the actual measurement results, thus more accurately reflecting the actual stress conditions within the tunnel.
- (4) The theoretical framework introduced in this research elucidates the attributes of internal force and deformation distributions within tunnel linings. Furthermore, it pinpoints the exact locations of peak internal forces and deformations, which are indispensable for evaluating the stability of tunnel linings. This lays a solid foundation for evaluating the structural integrity of tunnel linings.

REFERENCES

- Xu, S., Yu, M. (2014) Calculation of rock resistant factor in tunnel considering intermediate principal stress effect. *Chinese Journal of Rock Mechanics and Engineering*, 23(Supp.1), 4303-4305.
- [2] Gómez, J., Casas, R. J., Villalba, S. (2020) Structural health monitoring with distributed optical fiber sensors of tunnel lining affected by nearby construction activity. *Automation in Construction*, 117, 103261.
- [3] Wang, M., Lu, Z., Wan, W., Zhao, Y. (2021) A calibration framework for the microparameters of the DEM model using the improved PSO algorithm. *Advanced Powder Technology*, 32, 358-369.
- [4] Min, W., Wen, W, Zhao, Y. (2020) Prediction of uniaxial compressive strength of rocks from simple index tests using random forest predictive model. *Comptes Rendus Mécanique*, 348(1), 3-32.
- [5] Sudip, B., Sundar, S. K, Keshar, P. K., Thapa, U. J. (2023) Influence of tunnel shape on the shotcrete lining stress. *Journal of Physics: Conference Series*, 2629(1), 012015.
- [6] Tu, Z. (2006) Determination of rock resistant coefficient in road tunnel. Chinese Journal of Underground Space and Engineering, 2(3), 369-372.
- [7] Fan, W. (1962) Elastic resistance calculation of lining arch of upright wall railway tunnel. *Railway Standard Design*, (Supp.2), 9-30.
- [8] Tang, A., Li, D., Zhong, Z, Liu, X. (2005) Experimental research on rockmass elasticity resisting coefficient in Yantan Hydropower Station. *Chinese Journal of Rock Mechanics and Engineering*, 24(20), 3761-3765.
- [9] Lv, Y. (1981) A formula of rock resistant factor "K" in hydraulic pressure tunnel. *Chinese Journal of Geotechnical Engineering*, 3(1), 70-80.
- [10] Volodymyr, K, Volodymyr, P., Sofiia, K., Yevhenii, K. (2019) Numerical analysis of changing the force factors in temporary lining at the tunnel construction by the NATM. E3S Web of Conferences, 109, 00044.
- [11] Cai, X., Cai, Y., Cai, Y., Kang H. (2007) Calculation of resistance coefficient of adjoining rock for pressure tunnels considering effect of intermediate principal stress. *Chinese Journal of Geotechnical Engineering*, 28 (7), 1004-1008.
- [12] Cai, X., Lv, Y. (1984) Rock resist ant factor "K" in circle pressure tunnel by plastic hardening theory. *Chinese Journal of Geotechnical Engineering*, 6(3), 44-56.
- [13] Xianxing Wang, Wenhua Cui, Ye Tao, and Tianwei Shi, "Research on Deep Learning-based Object Detection Algorithm in Construction Sites," Engineering Letters, vol. 33, no. 1, pp1-12, 2025
- [14] Nam, S., Bobet, A. (2005) Liner stresses in deep tunnels below the water table. Tunnelling and Underground Space Technology incorporating Trenchless Technology Research, 21(6), 626-635.
- [15] Yuzhu Zhou, Dingyi Wei, Xin Lv, Zongzhi Wu, Zhiyong Shen, Chen Yu, Yang Mu, and Tiantian Li, "Research on the Transport Mechanism of Tunnel Dust Based on FLUENT," Engineering Letters, vol. 33, no. 3, pp520-529, 2025
- [16] Qin, S., Han, J. (1964) Determine elastic resistance distribution law of unsymmetrically loaded tunnel by asymptotic method. *Railway Standard Design*, (1), 10-14.